NASA TECHNICAL MEMORANDUM

NASA TM X-3322

NASA TM X-3322

ROUGH-TO-SMOOTH TRANSITION OF AN EQUILIBRIUM NEUTRAL CONSTANT STRESS LAYER

Earl Logan, Jr., and George H. Fichtl

George C. Marshall Space Flight Center
Marshall Space Flight Center, Ala. 35812

NATIONAL AERONAUTICS AND SPACE ADMINISTRATION • WASHINGTON, D. C. • DECEMBER 1975

1. REPORT NO.	2. GOVERNMENT ACCESSION NO.	3. RECIPIENT'S CATALOG NO.
NASA TMX-3322		

4. TITLE AND SUBTITLE	5. REPORT DATE
Rough-to-Smooth Transition of an Equilibrium Neutral Constant Stress Layer	December 1975
	6. PERFORMING ORGANIZATION CODE
7. AUTHOR(S)	8. PERFORMING ORGANIZATION REPORT #
Earl Logan, Jr.,* and George H. Fichtl	M158
9. PERFORMING ORGANIZATION NAME AND ADDRESS	10. WORK UNIT NO.
George C. Marshall Space Flight Center Marshall Space Flight Center, Alabama 35812	11. CONTRACT OR GRANT NO.
	13. TYPE OF REPORT & PERIOD COVERED
12. SPONSORING AGENCY NAME AND ADDRESS	Technical Memorandum
National Aeronautics and Space Administration Washington, D. C. 20546	14. SPONSORING AGENCY CODE

15. SUPPLEMENTARY NOTES

Prepared by Space Sciences Laboratory, Science and Engineering

*Arizona State University, Tempe, Arizona

16. ABSTRACT

The purpose of the research on the rough-to-smooth transition of an equilibrium neutral constant stress layer is to develop a model for low-level atmospheric flow over terrains of abruptly changing roughness, such as those occurring near the windward end of a landing strip, and to use the model to derive functions which define the extent of the region affected by the roughness change and allow adequate prediction of wind and shear stress profiles at all points within the region. A model consisting of two bounding logarithmic layers and an intermediate velocity defect layer is assumed, and dimensionless velocity and stress distribution functions which meet all boundary and matching conditions are hypothesized. The functions are used in an asymptotic form of the equation of motion to derive a relation which governs the growth of the internal boundary layer. The growth relation is used to predict variation of surface shear stress, and the associated wind and stress profiles along the new surface agree adequately with experimental wind profiles obtained in field studies.

17. KEY WORDS	18. DISTRIBUTION STATEMENT
	Category 47

19. SECURITY CLASSIF. (of this report)	20. SECURITY CLASSIF. (of this page)	21. NO. OF PAGES	22. PRICE
Unclassified	Unclassified	19	$3.00

For sale by the National Technical Information Service, Springfield, Virginia 22161

FOREWORD

The research reported herein was motivated by the need to understand the structure of the atmospheric boundary layer over airports for aircraft safety applications. This is one in a series of reports on low-level atmospheric flows as related to aeronautical operations published by the Aerospace Environment Division, Space Sciences Laboratory, NASA-Marshall Space Flight Center. The support for this research was provided by Mr. John Enders of the Aviation Safety Technology Branch, Office of Aeronautics and Space Technology in NASA Headquarters, and by the MSFC Summer Faculty Program.

TABLE OF CONTENTS

LIST OF ILLUSTRATIONS

LIST OF SYMBOLS

b	=	dimensionless ratio λ/δ_o
c	=	dimensionless constant
erf	=	error function
F	=	velocity defect function for IBL
G	=	shear stress difference function
h	=	height of Ekman layer
IBL	=	internal boundary layer
k	=	von Karman constant = 0.4
M	=	logarithm of ratio z_{oi}/z_o
r	=	dimensionless ratio δ_i/z_o
u^+	=	nondimensional horizontal component of mean wind
u	=	horizontal component of mean wind
u_o	=	mean wind velocity at $z = \delta_o$
u_i	=	mean wind velocity at $z = \delta_i$
u_b	=	mean wind velocity at $z = \lambda$
u_{*oi}	=	surface friction velocity upwind of discontinuity
u_{*o}	=	surface friction velocity downwind of discontinuity
x	=	horizontal coordinate, $x = 0$ at discontinuity

LIST OF SYMBOLS (Concluded)

z	=	vertical coordinate, $z = 0$ at surface of earth
z_{o1}	=	roughness length upwind of discontinuity
z_o	=	roughness length downwind of discontinuity
β	=	dimensionless ratio δ_i / δ_o
δ_i	=	thickness of IBL
δ_o	=	thickness of outer layer of IBL
η	=	dimensionless ratio z/δ_o
λ	=	thickness of sublayer of IBL
Λ	=	dimensionless coefficient
ξ	=	argument of error function
τ	=	shear stress
τ_{o1}	=	surface shear stress upwind of discontinuity
τ_o	=	surface shear stress downwind of discontinuity

TECHNICAL MEMORANDUM X-

ROUGH-TO-SMOOTH TRANSITION OF AN EQUILIBRIUM NEUTRAL CONSTANT STRESS LAYER

I. INTRODUCTION

The purpose of the research reported herein is to develop a model of a low-level atmospheric flow over a terrain of changing roughness length. A flow of this kind is found at the windward end of landing strips as the wind blows onto the relatively smooth surface of the strip from the relatively rough surface of the surrounding terrain. The work involves use of the proposed model to derive functions which define the extent of the region and allow the calculation of wind and shear stress profiles at all points within the affected region.

Elliott [1] was one of the first to study the change of terrain problem. He predicted that the thickness δ_i of the region affected by the change in roughness length increases with the 4/5-power of distance x from the discontinuity; i.e., with fetch. Elliott refers to the region of the flow disturbed by the discontinuity as the internal boundary layer (IBL). Other investigators have pursued the problem using various models for the internal boundary layer; e.g., Panofsky and Townsend [2-5], Taylor [6], Peterson [7], and Rao, Wyngard, and Cote [8]. Plate [9] has reviewed work done prior to 1971 on the internal boundary layer problem. The most recent studies utilize computer methods, together with a suitable turbulence closure model, to solve the governing equations.

A few investigators have studied the problem experimentally in wind tunnels. The earliest experimentation was done by Jacobs [10], and the latest was accomplished by Antonia and Luxton [11]. The latest field data were reported by Bradley [12]. Fair agreement has been obtained between experimental data and theoretical predictions.

The technique of asymptotic matching in conjunction with assumed scaling laws shall be used to extract as much information as possible from the equations of motions about the flow of concern. The motivation for this is to avoid lengthy and complicated numerical solution

methods which tend to mask the physics of the problem. The technique of asymptotic matching permits one to capture the physics of the problem, extract basic needed information, and avoid the negative aspects of numerical methods.

II. PROPOSED FLOW MODEL

The present investigation deals with the transition region occurring in a neutral constant stress layer due to an abrupt change in surface roughness, the line of the discontinuity being normal to the direction of the wind. It is assumed that the surfaces are covered with uniformly distributed roughness elements (i.e., small obstacles or protrusions) the height of which may be characterized by the scale z_o (roughness length). The flow is assumed to be steady, two-dimensional, and incompressible, with neutral hydrostatic stability prevailing throughout the entire layer. The approach that is used in the analysis is similar to that of Clauser [13] in his study of the turbulent boundary layer and of Csanady [14] and Blackadar and Tennekes [15] in their investigations of turbulent Ekman layers.

Blackadar and Tennekes [15] and many others have shown that the wind profile in the equilibrium surface layer upwind of the discontinuity is given by

$$\frac{u}{u_{*o1}} = \frac{1}{k} \ln \frac{z}{z_{o1}} \quad . \tag{1}$$

This equilibrium wind profile is represented schematically in Figure 1. Panofsky [16] states that the thickness of this surface, or logarithmic layer of the atmosphere, is of the order of 30 meters and that the Coriolis forces may be neglected in this layer.

Previous investigators assumed that an internal boundary layer is formed above the smooth surface (roughness length of z_o) and that it grows with increasing distance from the discontinuity at $x = 0$. In Figure 1 two regions are defined by a curve emanating from the origin; i.e.,

$$z = \delta_i(x) \quad , \tag{2}$$

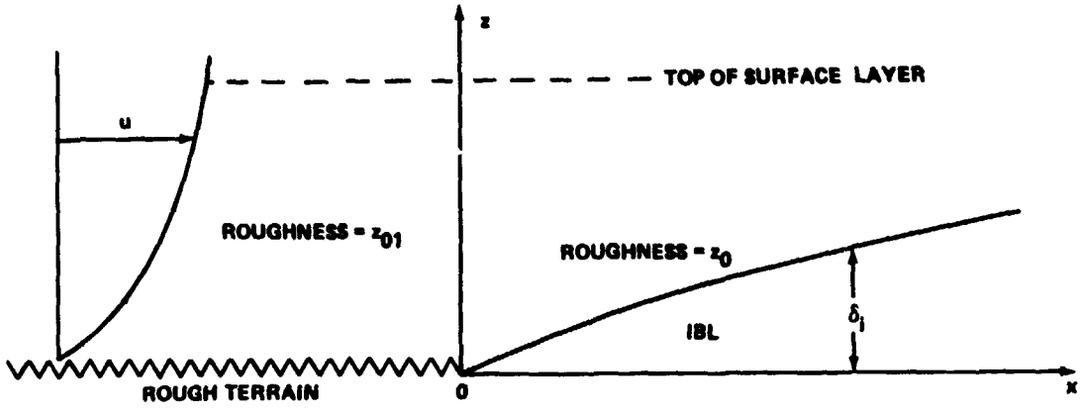

Figure 1. Development of an internal boundary layer for transition of flow from rough to smooth terrain.

which forms a surface above which the wind profile is described by equation (1) and below which the wind profile is undergoing transition to a new equilibrium profile given by

$$\frac{u}{u_{*o}} = \frac{1}{k} \ln \frac{z}{z_o} \quad . \tag{3}$$

The fetch x corresponding to the achievement of this condition is represented mathematically as $x \to \infty$. Equation (3) is of the same form as equation (1) and differs only in roughness length and velocity scale, z_o and u_{*o}, respectively.

A deficiency of the model of the flow as depicted in Figure 1 is that it does not provide for a gradual change of slope of the wind profile across the surface $\delta_i(x)$. One can easily verify that the velocity gradient $\partial u/\partial z$ obtained from differentiating equation (1) is not equal to that obtained from differentiation of equation (3). Thus, although wind may be specified as continuous at the boundary of the two regions, the derivatives are not continuous across this boundary.

To circumvent this difficulty it is proposed that the IBL be modeled as before but that an intermediate or matching region be

inserted between the two logarithmic regions as indicated in Figure 2.

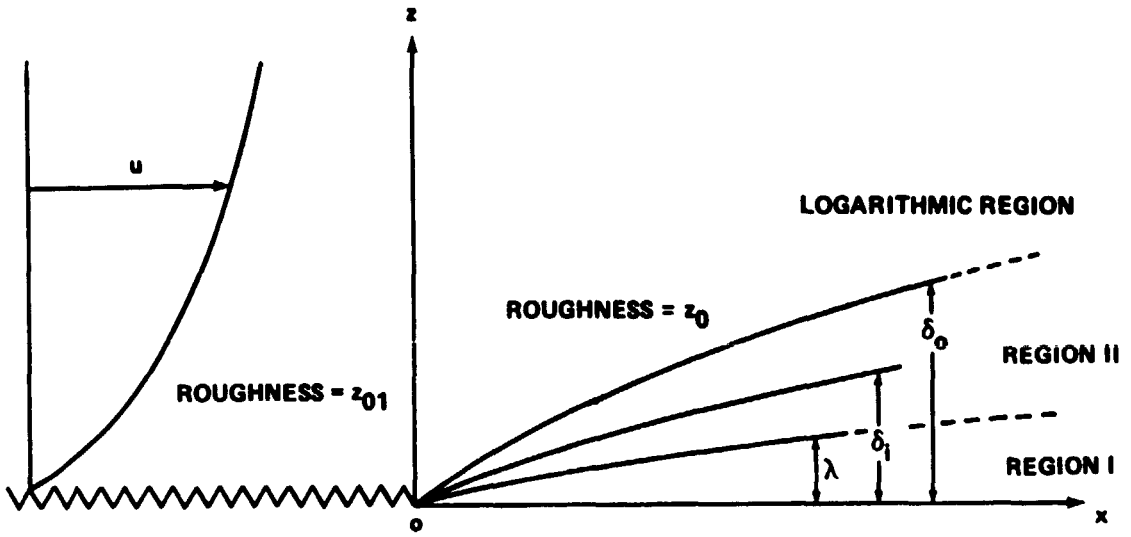

Figure 2. Sublayers of the internal boundary layer of proposed model.

The layer denoted as region I is the logarithmic layer in contact with the smooth surface. In region I the profile conforms to equation (3), with u_{*o} a function of x. The thickness of this layer is denoted by λ, with $\lambda < \delta_i$. Region II is the new intermediate layer of thickness $\delta_o - \lambda$ in which a gradual transition from one logarithmic wind profile to the other is accomplished. A velocity defect law is hypothesized for region II. Along the surface defined by $z = \delta_o$, it is assumed that complete matching to the external flow, governed by equation (1), has been accomplished, including wind, stress, and their derivatives.

The thickness δ_i of the internal boundary layer as previously defined and as depicted in Figure 1 is intermediate between the outer layer defined by the surface $z = \delta_o(x)$ and the sublayer defined by the surface $z = \lambda(x)$. Along the surface $z = \delta_i(x)$ the wind velocity u is given by

$$\frac{u_i}{u_{*o1}} = \frac{1}{k} \ln \frac{\delta_i}{z_{o1}} \quad . \tag{4}$$

This means that δ_i defines the surface below which the flow has accelerated relative to the original equilibrium profile given by equation (1). Continuity requires that the region defined by $\delta_i < z < \delta_o$ contain a flow which has decelerated relative to the original equilibrium profile.

Thus, the proposed model includes three length scales; viz., λ, δ_i, and δ_o, and three velocity scales; viz., u_{*o1}, u_*, and u_{*o}. These scales will be utilized in the next section to develop suitable similarity functions for wind and shear stress.

III. PROPOSED SIMILARITY FUNCTIONS

Townsend [3] found that similarity is possible in disturbed boundary layers if the disturbed layer is thin compared with the thickness of the boundary layer and if the roughness length is small compared with the thickness of the disturbed layer. Similarity may be assumed in the present problem if it is required that $\delta_i << h$ (where h is the thickness of the atmospheric boundary layer) and $z_o << \delta_i$, which are clearly valid except very close to and far from the origin.

Two functions are defined: the velocity defect function $F(\eta)$, which applies only to the intermediate layer (region II in Figure 2), and the shear stress function $G(\eta)$, which applies to the lower logarithmic layer (region I) as well as the intermediate layer. The velocity defect function is defined as

$$F(\eta) = \frac{u - u_i}{u_*} \quad , \tag{5}$$

with the dimensionless height above the surface defined as

$$\eta = \frac{z}{\delta_o} \quad . \tag{6}$$

The velocity u_i is the velocity on the surface defined by $z = \delta_i(x)$ and is calculated from equation (4). Friction velocity u_* in equation (5) is not the value at the surface but is a variable function of height z and fetch x. It is dependent on surface stress u^2_{*o}, a function of fetch only, and the shear stress function $G(\eta)$, which is defined as

$$G(\eta) = \frac{u_*^2 - u_{*o1}^2}{u_{*o}^2 - u_{*o1}^2} \tag{7}$$

and which clearly indicates the relationship between u_* and $G(\eta)$.

The nature of the similarity functions defined in equations (5) and (7) can be determined from a consideration of the boundary and matching conditions to which they must conform. The most obvious of these conditions are written first; i.e., those for which the function is zero or unity.

The function $F(\eta)$ is zero when the velocity u equals the velocity u_i on the surface defined by $z = \delta_i(x)$. The height of this surface is expressed nondimensionally as

$$\beta = \frac{\delta_i}{\delta_o} \quad . \tag{8}$$

Thus, the condition at this surface can be written as

$$F(\beta) = 0 \quad . \tag{9}$$

The function $G(\eta)$ is zero at the outer portion of region II where the shear stress must approach the upstream value τ_{o1}, which is the value of shear stress found at all heights in the equilibrium layer upstream of the discontinuity. This condition occurs at the height $z = \delta_o$ and is written as

$$G(1) = 0 \quad . \tag{10}$$

In the region above region II the shear stress is constant; therefore,

$$\frac{\partial \tau}{\partial z} = 0 \quad \text{for} \quad z \geq \delta_o \quad . \tag{11}$$

The resulting condition for the shear stress functio is

$$G'(1) = 0 \quad . \tag{12}$$

Similarly, in the lower part of the internal boundary layer; i.e., in region I,

$$G'(\eta) = 0 \quad \text{for} \quad \eta \leq b \quad , \tag{13}$$

where

$$b \equiv \frac{\lambda}{\delta_o} \quad . \tag{14}$$

Conditions at the extremities of region I may be written as

$$G'(b) = 0 \tag{15}$$

and

$$G'(0) = 0 \quad . \tag{16}$$

In the region I the stress function is unity since $\tau = \tau_o$ throughout the layer. Thus

$$G(\eta) = 1 \quad \text{for} \quad \eta \leq b \quad . \tag{17}$$

Thus, all the boundary and matching conditions on the stress function are included in equations (10) through (17). Additional conditions on the

velocity defect function $F(\eta)$ will be sought next.

At the outer limit of region II $u = u_o$, and equation (7) becomes

$$F(1) = -\frac{1}{k} \ln \beta \ , \tag{18}$$

where β is obtained from equation (8), u_i from equation (4), and u_o from

$$\frac{u_o}{u_{*o1}} = \frac{1}{k} \ln \frac{\delta_o}{z_{o1}} \ . \tag{19}$$

In order that the flow be self-preserving; i.e., that the function $F(\eta)$ not depend on fetch x, it is required that $F(1)$ = constant. This requirement imposed on equation (18) implies that β is at most a function of z_o/z_{o1}, which must be determined through experiments. The parameter β will be determined later for a particular example. A condition on the derivative $F'(1)$ may be obtained by matching derivatives at the juncture of region II and the upper logarithmic region. Equating expressions for $\partial u/\partial z$ obtained from differentiation of equations (1) and (5) results in the condition

$$F'(1) = \frac{1}{k} \ . \tag{20}$$

Next the interfacial conditions as $z \to \lambda$ ($\eta \to b$) are considered. Again, the derivatives are matched, with the following result:

$$F'(b) = \frac{1}{kb} \ . \tag{21}$$

Similarity requires that b, like β, is at most a function of z_o/z_{o1}, which must be determined by experiment. Its value is to be determined later for a particular case.

At this point a tentative velocity defect function is constructed which satisfies all of the necessary conditions for matching at the upper and lower bounds of region II; these conditions were given previously as equations (9), (18), (20), and (21). A suitable function for the region of velocity defect is

$$F(\eta) = \frac{1}{k} \ln\left(\frac{\eta}{\beta}\right) \quad , \tag{22}$$

and this function can be utilized to determine velocity distribution in region II after the growth law governing δ_i and the constant β are determined. The function given by equation (22) can be established via asymptotic considerations by demanding that the vertical gradient of u given by equation (3) as $z \to \infty$ and the vertical gradient of u given by equation (5) as $z \to 0$ merge together in an overlap region in which both formulations given by equations (3) and (5) are valid. This procedure assumes that $z \partial u_* / \partial z$ becomes small in comparison to $\eta \partial F / \partial \eta$ as $z \to 0$

Equation (22) may be utilized to derive a relationship between surface friction and internal boundary layer thickness. At the outer interface of region I

$$F(b) = \frac{u_b - u_i}{u_{*o}} \quad . \tag{23}$$

Substitution for u_i from equation (4) and for u_b from equation (3) with $z = \lambda$ leads to

$$\ln\left(\frac{\delta_i}{z_{o1}}\right) = \frac{M}{\frac{u_{*o1}}{u_{*o}} - 1} \quad , \tag{24}$$

where

$$M \equiv \ln\left(\frac{z_{o1}}{z_o}\right) \quad . \tag{25}$$

The utility of equation (24) will be demonstrated later.

The required stress function must satisfy the matching conditions given by equations (10), (12), (15), (16), and (17). Figure 3 depicts the shape of the required function as determined from the conditions listed above. An error function satisfies all matching conditions and is used to construct the stress function as is described below. The general form of the function is taken to be

$$G(\eta) = \Lambda \text{ erf } (\xi) + C \tag{26}$$

where the argument ξ is a function of η.

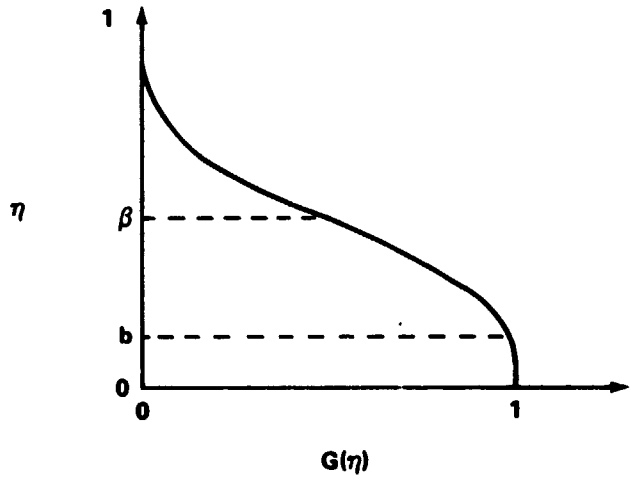

Figure 3. Schematic of properties of the nondimensional stress function $G(\eta)$.

Let $\eta = \beta$ be chosen to be the point of inflection; i.e., the maximum absolute value of slope $G'(\eta)$. This choice follows from a consideration of the terms of the equation of motion which governs flow in region II; i.e.,

$$u \frac{\partial u}{\partial x} + w \frac{\partial u}{\partial z} = \frac{\partial \tau}{\partial z} \quad . \tag{27}$$

It can be shown from equation (7) that the stress gradient is proportional to $G'(\eta)$. Equation (27) shows a direct dependence of stress gradient upon convective acceleration. Since the surface $z = \delta_i(x)$ separates regions of net positive and negative acceleration, it is plausible that fluid in the vicinity of that surface experiences the largest accelerations and, hence, the largest stress gradients. Since maximum stress gradient implies maximum absolute value of $G'(\eta)$, then $\eta = \beta$ corresponds to the maximum value of the derivative of the error function; i.e., $\xi = 0$ at $\eta = \beta$.

To construct the argument of ξ, cognizance is taken of the requirements stated in equations (12) and (15). The derivative of the error function is approximately zero when $|\xi| > 2$, where the error function itself is approximately unity. Choosing $|\xi| = 4$ for $\eta = b$ and $\eta = 1$ and substituting these values in equation (26) enables a determination of the constants C and Λ. To satisfy the conditions $\xi = 4$ at $\eta = b$ and $\xi = 0$ at $\eta = \beta$, the argument

$$\xi = \frac{4\,(\beta - \eta)}{\beta - b} \tag{28}$$

is selected. Substituting $\xi = -4$ at $\eta = 1$ into equation (28) gives the relation between β and b; viz.,

$$\beta = \frac{1}{2}\,(b + 1) \quad . \tag{29}$$

Substituting the above results into equation (26) yields the following expression for the shear stress function:

$$G(\eta) = \frac{1}{2}\,\mathrm{erf}\left[\frac{4\,(1 + b - 2\eta)}{1 - b}\right] + \frac{1}{2} \quad . \tag{30}$$

The constant b remains undetermined, and experimental data must be utilized to determine its value. Only one point of data is required, as will be demonstrated in the next section.

IV. DISTRIBUTION OF IBL THICKNESS AND SURFACE SHEAR STRESS

In this section a relationship between the thickness δ_i of the IBL and the fetch x, i.e., the IBL growth law, is derived. This is obtained by integrating an asymptotic form of equation (27), the equation of motion. The terms are simplified by letting $\eta = \beta$ and $x \to 0$. This results in an easily integrated differential equation since $F(\beta)$, $F'(\beta)$ and u_{*_o} are easily inferred from equations (22) and (24) for the limiting values considered. The surface friction velocity approaches zero in the limit as $x \to 0$, which is consistent with equation (24). In view of this, it is plausible that u_* at $\eta = \beta$ will approach zero as the discontinuity is approached; however, equation (7) indicates that a minimum value of u_* is approached but not a zero value, because equation (7) is not valid at the roughness discontinuity. Nevertheless, in reducing the equation of motion it is assumed that $u_* \to 0$ as $x \to 0$. A physical justification for this assumption is that the velocity gradient,

$$\frac{\partial u}{\partial z} = \frac{u_* F'(\beta)}{\delta_o} = \frac{u_*}{k\delta_i} \quad , \tag{31}$$

is expected to be small initially at $\eta = \beta$; i.e., in the vicinity of the juncture of the new and old velocity profiles. This is expected because of the acceleration of the fluid inside the IBL relative to that above the IBL. Equation (31) requires a small value of u_* as δ_i shrinks near the origin.

The above assumptions reduce equation (27) to the simplified differential equation

$$\delta_i' \ln\left(\frac{\delta_i}{z_{o_1}}\right) = -k^2 \beta G'(\beta) \quad . \tag{32}$$

Integration of equation (32) results in the growth law,

$$r\,[\ln r - (1+M)] + e^{M} = \frac{-k^2 \beta G'(\beta)\, x}{z_o} \quad , \tag{33}$$

where

$$r \equiv \frac{\delta_i}{z_o} \quad . \tag{34}$$

The boundary condition that $r = e^{M}$ at $x = o$ was used to derive equation (33).

Equation (33) can be used to predict the growth of the internal boundary layer if the constant $\beta G'(\beta)$ is determined from experimental data. From Bradley's data [12], valid for M = 4.83, as plotted in Figure 12 of Rao, Wyngaard, and Cote [8],

$$\beta G'(\beta) = -1.918 \quad . \tag{35}$$

It should be kept in mind that this numerical result is only valid for a particular value of z_o / z_{o_1} or rather M = 4.83.

The resulting value from equation (36) may be used with equation (33) to predict internal boundary layer thickness at other fetches. A curve depicting the results of this calculation is shown in Figure 4 with Bradley's data for M = 4.83.

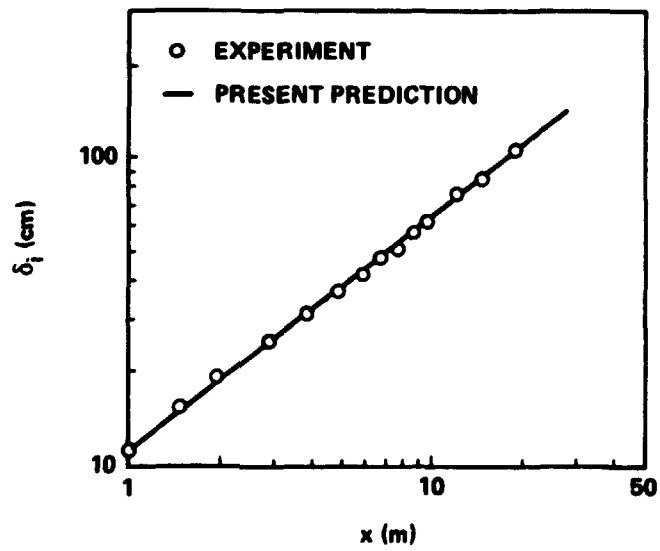

Figure 4. Growth of the internal boundary layer with fetch. The experimental data are those of Bradley [12].

Values of δ_i calculated from equation (33) can be utilized with equation (24) to determine surface stress as a function of fetch. The curve in Figure 5 shows the comparison of predicted surface stresses with experimental data from Bradley [12] and numerical predictions from Rao, Wyngaard, and Cote [8].

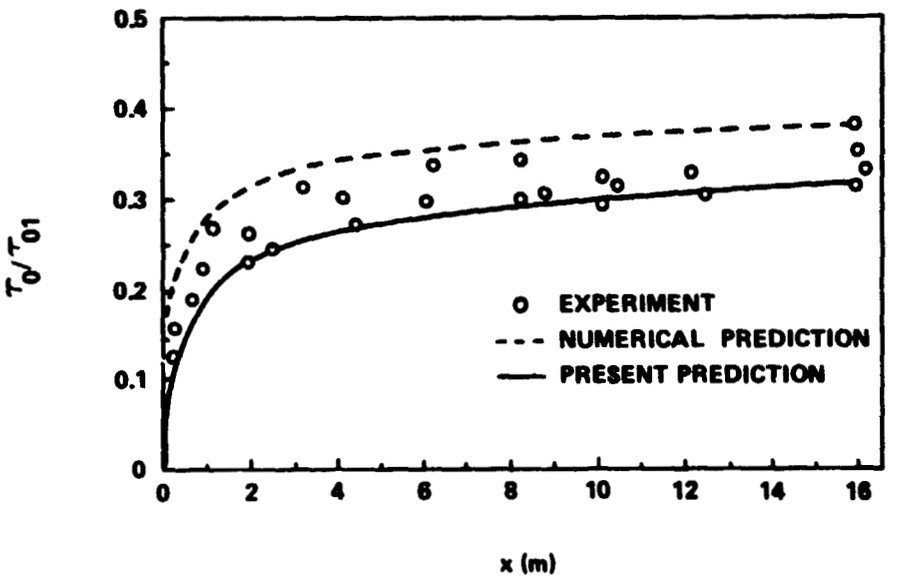

Figure 5. Nondimensional surface shear stress as a function of fetch. The experimental data are those of Bradley [12]. The numerical prediction of Rao, Wyngaard, and Cote [8] is indicated with the dashed curve. The prediction of the theory herein is indicated with the solid curve.

The results shown in Figures 4 and 5 indicate the degree of success achieved in the prediction of internal boundary layer growth and of surface shear stress variation with fetch. Agreement between theoretical prediction and experiment is achieved at all stations for which experimental data are available.

V. PREDICTION OF WIND AND SHEAR STRESS PROFILES IN IBL

The prediction of wind and shear stress profiles in the internal boundary layer following a discontinuity in surface roughness can be achieved through the use of the equations developed in previous sections. To achieve this, use is made of equations (22) and (30) in the form

$$F(\eta) = 2.5 \ln\left(\frac{8\eta}{5}\right) \tag{36}$$

and

$$G(\eta) = \frac{1}{2} \operatorname{erf}\left[\frac{4(5 - 8\eta)}{3}\right] + \frac{1}{2} \tag{37}$$

in which the values $b = 0.25$ and $\beta = 0.625$ have been substituted. The approximate value of b is obtained by differentiation of equation (26) and substitution of equation (35). The parameter β is evaluated with equation (29).

To calculate a wind profile in the internal boundary layer it is necessary to know the two roughness lengths and the surface stress upwind of the discontinuity. With this information δ_i is calculated from equation (33), u_{*_o} from equation (24), and u_i from equation (4). With these values calculated as indicated above, a set of quantities is calculated at each height z; for region II this procedure is carried out as follows: i) η is calculated from equation (6); ii) $G(\eta)$ is calculated from equation (37); iii) $u_*^2 (u_*^2 = \tau)$ is calculated from equation (7); iv) $F(\eta)$ is calculated from equation (36); and v) u is calculated from equation (5). This completes the method of calculating wind and shear stress profiles in region II; i.e., u - z and τ - z profiles, respectively. Outside region II the wind profile is determined from equation (1) for $z > \delta_o$ and from equation (3) for $z < \lambda$. Some results of this calculation are shown graphically in Figure 6 and are compared with the corresponding experimental data of Bradley [12].

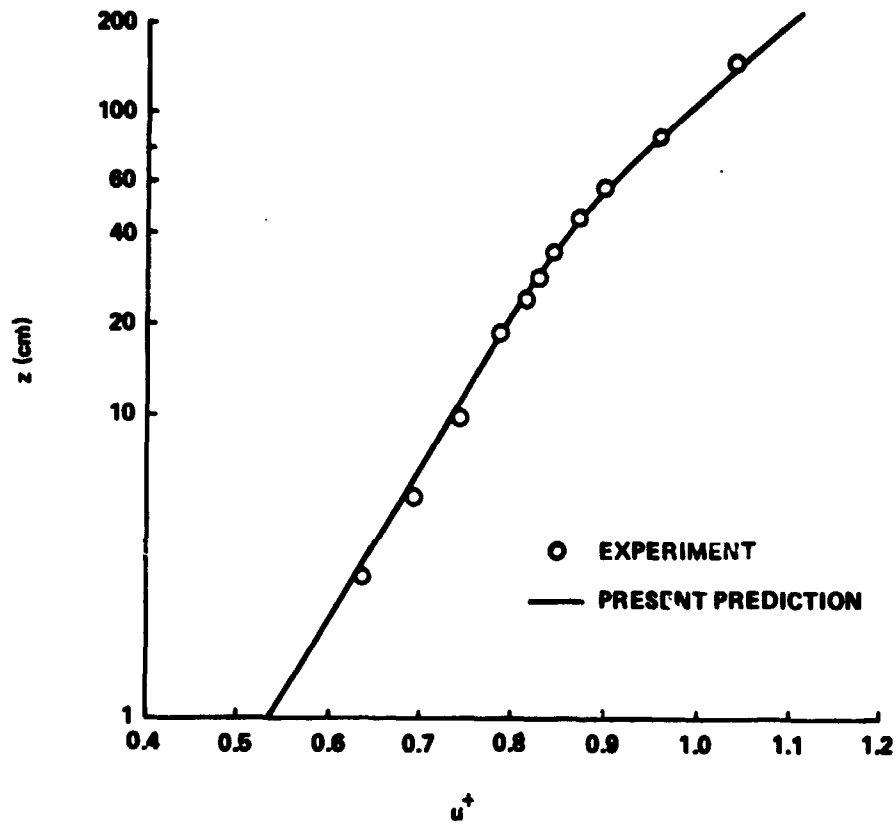

Figure 6. Nondimensional wind profile u^+ at x = 6.1 m for M = 4.83. The quantity $u^+ = u(z)/u(z = 112.5\ cm)$. The experimental data are those of Bradley [12].

It is evident from Figure 6 that the calculation method based on the proposed model is capable of producing reasonable predictions of wind profiles in the internal boundary layer associated with modification of the surface layer. Since the calculation of a wind profile requires use of the corresponding shear stress profile, the model is assumed to be valid for shear stress prediction as well.

VI. REFERENCES

1. Elliott, W. P.: The growth of the atmospheric internal boundary layer. Trans. Amer. Geophys. Union 39, 1048-1054, 1958.

2. Panofsky, H. A., and Townsend, A. A.: Change of terrain roughness and the wind profile. Quart. J. Roy. Meteor. Soc. 90, 147-155, 1964.

3. Townsend, A. A.: Self-preserving flow inside a turbulent boundary layer. J. Fluid Mech. 22, 773-797, 1965.

4. Townsend, A. A.: The response of a turbulent boundary layer to abrupt changes in surface conditions. J. Fluid Mech. 22, 799-822, 1965.

5. Townsend, A. A.: The flow in a turbulent boundary layer after a change in surface roughness. J. Fluid Mech. 26, 255-266, 1966.

6. Taylor, P. A.: The planetary boundary layer above a change in surface roughness. J. Atmos. Sci. 26, 432-440, 1969.

7. Peterson, E. W.: Modification of mean flow and turbulent energy by a change in surface roughness under conditions of neutral stability. Quart. J. Roy. Meteor. Soc. 95, 561-575, 1969.

8. Rao, K. S.; Wyngaard, J. C.; and Cote, O. R.: The structure of the two-dimensional internal boundary layer over a sudden change of surface roughness. J. Atmos. Sci. 31, 738-746, 1974.

9. Plate, E. J.: Aerodynamic Characteristics of Atmospheric Boundary Layers. U. S. Atomic Energy Commission, TID-25465, 1971, 190 pp.

10. Jacobs, W.: Transformation of turbulent velocity pr iles. Z. Angew. Math. Mech. 19, 87-100, 1939. (NACA-TM951)